

Improving Matrix Exponential for Generative AI Flows: A Taylor-Based Approach Beyond Paterson–Stockmeyer

J. Sastre^a, D. Faronbi^e, J.M. Alonso^b, P. Traver^e, J. Ibáñez^c, N. Lloret^d

Universitat Politècnica de València, Spain

^a*Instituto de Telecomunicaciones y Aplicaciones Multimedia*

^b*Instituto de Instrumentación para Imagen Molecular*

^c*Instituto de Matemática Multidisciplinar*

^d*Instituto de Diseño para la Fabricación y Producción Automatizada*

^e*Music and Audio Research Lab, New York University, New York, USA*

Abstract

The matrix exponential is a fundamental operator in scientific computing and system simulation, with applications ranging from control theory and quantum mechanics to modern generative machine learning. While Padé approximants combined with scaling and squaring have long served as the standard, recent Taylor-based methods, which utilize polynomial evaluation schemes that surpass the classical Paterson–Stockmeyer technique, offer superior accuracy and reduced computational complexity. This paper presents an optimized Taylor-based algorithm for the matrix exponential, specifically designed for the high-throughput requirements of generative AI flows. We provide a rigorous error analysis and develop a dynamic selection strategy for the Taylor order and scaling factor to minimize computational effort under a prescribed error tolerance. Extensive numerical experiments demonstrate that our approach provides significant acceleration and maintains high numerical stability compared to existing state-of-the-art implementations. These results establish the proposed method as a highly efficient tool for large-scale generative modeling.

Keywords: Matrix exponential, scaling and squaring, Taylor

*Corresponding author: jsastrem@upv.es. This work has been supported by the Generalitat Valenciana Grant CIAICO/2023/275.

1. Introduction

The computation of matrix functions, particularly the matrix exponential, has been extensively studied due to its wide range of applications in science and engineering [1, 2]. Among the various numerical methods developed, Padé approximants have traditionally been favored over Taylor series due to their superior efficiency for comparable accuracy [23]. However, despite its widespread adoption, the standard Padé-based approach often incurs unnecessary computational overhead. Recent work, such as [26], has demonstrated that truncated Taylor series can represent a simpler and more efficient alternative, frequently yielding substantial speedups over the Padé-based scaling and squaring implementations found in standard software routines like MATLAB's `expm`.

In fact, recent advances have shown that Taylor-based methods can outperform Padé approximants in both accuracy and efficiency. The Taylor algorithm introduced in [3] improved upon classical Padé-based methods [23], while subsequent research [4, 5, 6] refined the associated error analysis and reduced computational costs.

A significant breakthrough in this area was the development of advanced matrix polynomial evaluation techniques [9] that surpass the classical Paterson–Stockmeyer method [13]. These techniques, predicated on structured multiplications and linear combinations of matrix polynomials, enable higher-order Taylor approximations with reduced computational effort. For instance, the method presented in [22] introduced $m+$ approximations, where the first m terms match the Taylor series exactly, while additional terms are optimized to enhance accuracy. These schemes, such as the $m = 15+$ case introduced in [9, Ex. 5.1], achieve greater precision than standard Taylor polynomials of equivalent computational cost. Furthermore, recent optimizations for determining evaluation formula coefficients [18] have shown promising results for broader matrix function computations [18, 19].

The cost of these polynomial approximation methods is dominated by matrix multiplications, denoted by M . In practice, these operations scale as $\mathcal{O}(n^3)$ for $n \times n$ matrices, whereas matrix additions and scalar multiplications

are of order $\mathcal{O}(n^2)$. In rational methods, matrix inverses are computed by solving linear systems, the cost of which can also be expressed in terms of matrix products as [12, App. C]:

$$D \approx \frac{4}{3}M. \quad (1)$$

Consequently, throughout this paper, the cost of both rational and polynomial approximations is quantified in terms of M .

Table 1 compares the cost and achievable approximation orders of various state-of-the-art methods, including Padé approximants, Paterson–Stockmeyer evaluation, and mixed rational-polynomial schemes [11, 22, 14]. The results highlight the superior efficiency of modern polynomial evaluation strategies, which facilitate higher-order approximations using fewer matrix multiplications.

In this paper, we propose an optimized implementation of the matrix exponential based on the evaluation methods described in [9]. Our approach is specifically tailored for the high-throughput requirements of Generative AI flows, where the repeated evaluation of the matrix exponential often constitutes a primary computational bottleneck. Unlike traditional software routines optimized for fixed IEEE precision using pre-computed thresholds [21, 14, 22, 15], or flexible implementations that depend on external specialized libraries [16], we introduce a self-contained framework that dynamically selects the Taylor order and scaling factor for any user-defined tolerance ε . While previous dynamic methods have utilized classical Paterson–Stockmeyer schemes with more complex scaling strategies [17], the proposed algorithm leverages higher-order polynomial evaluations with a simplified operational logic. This provides a portable, library-independent solution that balances numerical stability with significant reductions in execution time for large-scale generative models.

Throughout this manuscript, $\mathbb{C}^{n \times n}$ denotes the set of complex matrices of size $n \times n$, I denotes the identity matrix for this set, $\rho(A)$ is the spectral radius of matrix A , and \mathbb{N} denotes the set of positive integers. The matrix norm $\|\cdot\|$ denotes any subordinate matrix norm; in particular $\|\cdot\|_1$ is the 1-norm. The symbols $\lceil \cdot \rceil$ and $\lfloor \cdot \rfloor$ denote the smallest following and the largest previous integer, respectively.

This paper begins in Section 2 by reviewing the role and challenges associated with the matrix exponential in generative flow models. Section 3 introduces the proposed computational methodology, which includes new

Polynomial evaluation cost	$3M$	$4M$	$5M$	$6M$	$7M$
Approx. order m Paterson–Stockmeyer [13]	6	9	12	16	20
Approx. order m [14]	8	12	18	22	—
Approx. order m [22]	8	15+	21+	24	30
Mixed rational polynomial approx. cost	$3.33M$	$4.33M$	$5.33M$	$6M$	$7M$
Approx. order from method [11, Tab. 3]	9	12	16	21	28
Padé evaluation cost	$3.33M$	$4.33M$	$5.33M$	$6.33M$	$7.33M$
Approx. order Padé method [23, Tab. 2.2]	6	10	14	18	26

Table 1: Cost and available order of approximation with the polynomial evaluation methods from Paterson–Stockmeyer [13], Sastre–Ibáñez–Defez [22, Sec. 3], Bader–Blanes–Casas [14, Sec. 4], the mixed rational and polynomial approximation method from Sastre [11, Tab. 3] and the Padé approximation method from Higham [23, Tab. 2.2].

evaluation formulas for the Taylor matrix polynomial approximation (Subsection 3.1) based on [9, 10], a discussion of the scaling and squaring error analysis (Subsection 3.2), and the complete algorithmic procedure (Subsection 3.3). Subsequently, Sections 4 and 5 provide the numerical results that assess the algorithm’s performance, and Section 6 presents the conclusions.

2. The matrix exponential for generative flows

2.1. Generative models

In recent years, generative models have become very popular. They aim to use training data to learn the probability distribution of a dataset. The resulting model of the distribution can be sampled to obtain new data points according to their estimated probability. This has proven useful in a variety of tasks, including music generation [27, 28], denoising [29], and representation learning [30].

There are a variety of approaches to train these probabilistic models. Generative adversarial networks (GANs) [31] train two models with adversarial objectives. Variational Autoencoders (VAEs) [32] take a bayesian approach to modelling the data with a prior. Denoising diffusion models [33] aim to model a denoising process (sometimes called score matching) to progressively transform a noise signal into a data point. While these techniques have all been applied succesfully to generative tasks, they unfortunately lack invertibility. Flow generative models were developed to have an invertible mapping from a noise distribution to a data distribution.

2.2. Generative flows

For random variable $x \in \mathbb{R}^n$ representing data with probability distribution $p(x)$ and random variable $z \in \mathbb{R}^n$ with a known probability density function $p(z)$, generative flows aim to model an invertible transformation of x into $z = f(x)$. By the change of variable formula, the relationship between $p(x)$ and $p(z)$ is:

$$\log p(x) = \log p(z) + \log \left| \frac{\delta f(x)}{\delta x} \right|, \quad (2)$$

where $\frac{\delta f(x)}{\delta x}$ is the Jacobian of f . Assume that there are k number of invertible functions. Then, the log-likelihood of x is given by

$$\log p(x) = \log p(z) + \sum_{i=1}^k \log \left| \frac{\delta h_i}{\delta h_{i-1}} \right|, \quad (3)$$

where $h_i = f_i(h_{i-1})$.

In generative flow models [25], the transformation function f is typically implemented as a composition of invertible functions, often parameterized as $f = W_m \phi(W_{m-1} \phi(\dots \phi(W_1 x)))$, where W_i are weight matrices and ϕ is a strictly monotonic activation function. Ensuring invertibility of each W_i during training is challenging, and Calculating the determinant of a general matrix is computationally intensive, with a complexity of $O(n^3)$ for an $n \times n$ matrix. A common workaround is to constrain W_i to be triangular, which simplifies determinant computation but limits expressiveness and parallelizability.

Over the years, there have been multiple approaches to modeling normalizing flows that address this computationally expensive log determinant problem. One solution is to model f autoregressively [40], calculating the determinant in $\mathcal{O}(n)$ time. Contractive residual layers have been used to implement invertible transforms [42]. They result in unbiased density estimators at the cost of long computation time. Multiple approaches use coupling layers [39, 41] to implement unbiased reversible transformations with a triangular matrix for a traceable determinant calculation.

One approach [25] proposed replacing each weight matrix W_i with its matrix exponential e^{W_i} . This guarantees invertibility, improves expressiveness over triangular matrices, and enables efficient computation of both the inverse and the log-determinant. Specifically, the inverse is given by $(e^W)^{-1} = e^{-W}$,

and the log-determinant simplifies to $\log \det(e^W) = \text{Tr}(W)$, reducing the computational cost from $\mathcal{O}(n^3)$ to $\mathcal{O}(n)$.

The matrix exponential maps $\mathbb{M}_n(\mathbb{R})$ to $\text{GL}_n(\mathbb{R})^+$, the group of invertible matrices with positive determinant. Although not surjective, its image is rich enough for practical purposes, and any matrix in $\text{GL}_n(\mathbb{R})^+$ can be expressed as a product of matrix exponentials. This makes the matrix exponential a powerful tool for constructing expressive and invertible neural architectures in generative modeling [25].

Algorithm 1 Algorithm for Computing Matrix Exponential

Require: Weight matrix W , error tolerance ε

Ensure: Matrix exponential e^W

```

1: Choose the smallest non-negative integer  $s$  such that  $\|W\|_1/(2^s) < \frac{1}{2}$ 
2:  $W = W/(2^s)$ 
3:  $X = I$ 
4:  $Y = W$ 
5:  $k = 2$ 
6: while  $\|Y\|_1 > \varepsilon$  do
7:    $X = X + Y$ 
8:    $Y = W \cdot Y/k$ 
9:    $k = k + 1$ 
10: end while
11: for  $i = 1$  to  $s$  do
12:    $Y = Y \cdot Y$ 
13: end for
14: return  $Y$ 

```

For the sake of completeness the algorithm for the computation of the matrix exponential described in [25, Sec. 3.2] is reproduced here as Algorithm 1. It relies on the matrix exponential Taylor series expansion [2, Sec. 3], denoted by $T_m(W)$ and given by

$$T_m(W) = \sum_{i=0}^m \frac{W^i}{i!}, \quad (4)$$

where terms are successively summed until the norm of the last term falls below a prescribed tolerance ε . This approach uses a forward absolute error criterion based on an error bound for the Taylor series remainder for

approximating the matrix exponential, denoted by $R_m(W)$ and given by

$$R_m(W) = e^W - T_m(W) = \sum_{i=m+1}^{\infty} \frac{W^i}{i!}, \quad (5)$$

which is bounded by [34]:

$$\|R_m(W)\|_1 \leq \frac{\|W\|_1^{m+1}}{(m+1)!} \left(\frac{1}{1 - \frac{\|W\|_1}{m+2}} \right). \quad (6)$$

Note that the truncated Taylor series is particularly well-suited for scenarios with limited computational resources, restricted access to external libraries or large-scale problems involving well-behaved matrices [26, p. 52]. According to [25, Sec. 3.2], the weight matrices in neural networks, denoted by W , are often small in norm such that $\|W\|_1$ is also small. This property makes the incorporation of the matrix exponential into neural network architectures computationally feasible. Exploiting the identity $e^W = (e^{W/2^s})^{2^s}$, in Algorithm 1 the matrix is first scaled to ensure that $\|W/2^s\|_1 < 1/2$, after which the exponential is computed and subsequently squared 2^s times. This scaling and squaring strategy further reduces the computational cost while maintaining numerical stability; see [25, Alg. 1]. The computational cost of evaluating a Taylor approximation of degree m using [25, Alg. 1], denoted by $T_m(A)$, is measured in terms of matrix multiplications. Let C_{orig} represent the cost of evaluating the unscaled Taylor polynomial in Algorithm [25, Alg. 1], which is given by

$$C_{\text{orig}} = m - 1. \quad (7)$$

When scaling is applied, the total cost becomes $(s + m - 1)M$, where s is the scaling parameter. As reported in [25, Sec. 6.4], a tolerance of $\varepsilon = 10^{-8}$ is used. Under this setting, the total number of matrix products, given by $s + m - 1$, does not exceed 11, with an average value of 9.28 observed during training [25, Tab. 6].

Cost (7) makes Algorithm 1 unsuitable for high-dimensional data [25, Sec. 3.2]. To address this limitation, a second method is proposed that combines matrix exponentials with neural networks, using a low-rank parameterization of the weight matrix $W = A_1 A_2$, where $A_1 \in \mathbb{R}^{n \times t}$ and $A_2 \in \mathbb{R}^{t \times n}$.

By defining $V = A_2 A_1$, and using the associative property of matrix multiplication, the matrix exponential e^W can be approximated via a truncated series expansion of V :

$$e^W \approx I + A_1 \left(\sum_{i=0}^m \frac{V^i}{(i+1)!} \right) A_2, \quad (8)$$

where the truncation error bound of the matrix series of V , denoted here by $R'_m(V)$, is given by (8) from [25, Sec. 3.2] reproduced here

$$\|R'_m(V)\|_1 = \left\| \sum_{i=m+1}^{\infty} \frac{V^i}{(i+1)!} \right\|_1 \leq \left(\frac{\|V\|_1^{m+1}}{(m+2)!} \right) \left(\frac{1}{1 - \frac{\|V\|_1}{m+3}} \right). \quad (9)$$

This reduces the computational cost to $\mathcal{O}(t^3)$ since $V \in \mathbb{R}^{t \times t}$. The rank of W is at most t , so choosing a smaller t improves efficiency but may reduce expressiveness. Thus, there is a trade-off between computational cost and model capacity.

The approximation method is similar to Algorithm 1, with modifications: set the scale coefficient $s := 0$, change line 4 to $Y := W/2$, and line 5 to $k := 3$ [25, Sec. 3.2].

While the cost of the algorithms proposed in [25, Sec. 3.2] represent a reasonable computational cost, further reductions are possible by optimizing the polynomial evaluation strategy.

3. Proposed method

Our implementation is specifically tailored for this generative flow setting. It builds upon efficient polynomial evaluation techniques, extending beyond the classical Paterson–Stockmeyer method as introduced in [9], to substantially reduce the number of matrix products required for a specified approximation order. Furthermore, the algorithm incorporates a dynamic procedure that optimally selects the Taylor series degree (m) and the scaling factor (s) to minimize the overall computational cost. This selection ensures that the error tolerance is strictly maintained, chosen to be no less than the unit roundoff (u) of the arithmetic used, while also strategically reducing the risk of overscaling [21, Sec. 1].

Numerical experiments confirm that our approach consistently achieves lower average computational costs than the baseline method in [25], particularly in the context of generative AI flows, where evaluations of thousands of matrix exponentials are required. This improvement translates into faster training times and reduced resource consumption, making our method suitable for large-scale machine learning applications.

c_1	$4.980119205559973 \times 10^{-3}$
c_2	$1.992047682223989 \times 10^{-2}$
c_3	$7.665265321119147 \times 10^{-2}$
c_4	$8.765009801785554 \times 10^{-1}$
c_5	$1.225521150112075 \times 10^{-1}$
c_6	$2.974307204847627 \times 10^0$

Table 2: Coefficients for the Taylor approximation of the matrix exponential of order $m = 8$, computed using formulas (13) and (14)

3.1. Evaluation formulas of the Taylor-based matrix exponential approximations

This work adopts the evaluation formulas from [22] to compute Taylor-based approximations for orders up to $m = 15+$. Table 1 demonstrates that these schemes significantly outperform the Paterson–Stockmeyer method; for a fixed computational budget, they achieve orders 8 and 15+, whereas the classical approach only reaches orders 6 and 9, respectively. Moreover, these schemes represent the most efficient approximations identified in Table 1, outperforming both the state-of-the-art Taylor [14] and Padé [23] methods. Although [22] also provides formulas for higher-order Taylor approximations, given the low error tolerance required in our application, these higher-order variants do not offer a reduction in computational cost and are therefore excluded from consideration. For completeness, the formulas corresponding to the selected approximation orders are reproduced below.

$$T_1(A) = A + I, \quad (10)$$

$$T_2(A) = A^2/2 + A + I, \quad (11)$$

$$T_4(A) = ((A^2/4 + A)/3 + I)A^2/2 + A + I, \quad (12)$$

$$y_{02}(A) = A^2(c_1A^2 + c_2A), \quad (13)$$

$$T_8(A) = (y_{02}(A) + c_3A^2 + c_4A)(y_{02}(A) + c_5A^2) + c_6y_{02}(A) + A^2/2 + A + I, \quad (14)$$

where the coefficients c_i , for $i = 1, 2, \dots, 6$, are listed in Table 2, rounded to IEEE double-precision floating-point arithmetic.

c_1	$4.018761610201036 \times 10^{-4}$	c_9	$2.224209172496374 \times 10^0$
c_2	$2.945531440279683 \times 10^{-3}$	c_{10}	$-5.792361707073261 \times 10^0$
c_3	$-8.709066576837676 \times 10^{-3}$	c_{11}	$-4.130276365929783 \times 10^{-2}$
c_4	$4.017568440673568 \times 10^{-1}$	c_{12}	$1.040801735231354 \times 10^1$
c_5	$3.230762888122312 \times 10^{-2}$	c_{13}	$-6.331712455883370 \times 10^1$
c_6	$5.768988513026145 \times 10^0$	c_{14}	$3.484665863364574 \times 10^{-1}$
c_7	$2.338576034271299 \times 10^{-2}$	c_{15}	1
c_8	$2.381070373870987 \times 10^{-1}$	c_{16}	1

Table 3: Coefficients of y_{02} , y_{12} , and y_{22} from equations (15)-(17) used in the Taylor-based approximation of the matrix exponential of order $m = 15+$.

$$y_{02}(A) = A^2(c_1A^2 + c_2A), \quad (15)$$

$$y_{12}(A) = (y_{02}(A) + c_3A^2 + c_4A)(y_{02}(A) + c_5A^2) + c_6y_{02}(A) + c_7A^2, \quad (16)$$

$$y_{22}(A) = (y_{12}(A) + c_8A^2 + c_9A)(y_{12}(A) + c_{10}y_{02}(A) + c_{11}A) \\ + c_{12}y_{12}(A) + c_{13}y_{02}(A) + c_{14}A^2 + c_{15}A + c_{16}I, \quad (17)$$

where the coefficients c_i , for $i = 1, 2, \dots, 16$, are listed in Table 3, also rounded to IEEE double-precision floating-point arithmetic.

Note that

1. $T_1(A)$ and $T_2(A)$ in (10) correspond to the direct Taylor evaluation formulas of orders 1 and 2, respectively, while $T_4(A)$ corresponds to the Paterson–Stockmeyer evaluation scheme [13] for order $m = 4$.
2. The cost of evaluating $T_8(A)$ using formulas (13) and (14) is $3M$: one multiplication for computing A^2 , one for evaluating (13), and one for evaluating (14). In contrast, computing the Taylor approximation of degree $m = 8$ using the original algorithm from [25, Alg. 1], as given by (7), requires $7M$, which is more than twice as expensive.
3. Recall that, in exact arithmetic, equations (15) and (16) from [22] show that $y_{22}(A)$ in (17) satisfies

$$y_{22}(A) = T_{15}(A) + b_{16}A^{16}, \quad (18)$$

and, therefore, the approximation remainder is given by

$$R_{15+}(W) = e^W - y_{22}(W) = \left(\frac{1}{16!} - b_{16} \right) W^{16} + \sum_{i=17}^{\infty} \frac{W^i}{i!}, \quad (19)$$

where, from (15)–(17), it can be shown that the coefficient is $b_{16} = c_1^4$. Using the value of c_1 from Table 3, we obtain

$$b_{16} = c_1^4 \approx 2.608368698098256 \times 10^{-14}. \quad (20)$$

This value differs from the exact Taylor coefficient $1/16!$ by a relative error of approximately $|b_{16} - 1/16!| \cdot 16! \approx 0.454$. Consequently, $y_{22}(A)$ provides a more accurate approximation than $T_{15}(A)$ in exact arithmetic, although it remains less accurate than the full Taylor approximation $T_{16}(A)$ as demonstrated in [22]. Approximations of this type are referred to in [22] as $T_{15+}(A)$. Similarly, in this case, the cost of evaluating $y_{22}(A)$ using formulas (15)–(17) is $4M$.

3.2. Error analysis

This section details the self-contained framework for the dynamic selection of the Taylor order m and the scaling parameter s . Unlike fixed-precision algorithms that rely on pre-computed thresholds for specific IEEE formats or error tolerances [21, 14, 22, 15], the proposed approach derives these parameters directly for a user-specified tolerance ε . By integrating advanced polynomial evaluation formulas into the error bound analysis, we achieve a more streamlined selection logic than previous dynamic methods [17].

In particular, we provide a refined version of the absolute error analysis from (6) specifically for nonnormal matrices. For such matrices, the relation (1.5) from [21] states that

$$\rho(A) \leq \|A^k\|^{1/k} \leq \|A\|, \quad k = 1, 2, \dots, \infty. \quad (21)$$

Consequently, the inequality

$$\|A^k\| \leq \|A\|^k, \quad k = 1, 2, \dots, \infty, \quad (22)$$

can be significantly strict, i.e., $\|A^k\| \ll \|A\|^k$, as discussed in [21, Sec. 1]. This property is exploited in [5, Th. 1.1] to derive tighter bounds for the matrix power series, ensuring efficiency without the overhead of overscaling. For completeness of the exposition, the theorem is reproduced below:

Theorem 1. *Let $h_l(x) = \sum_{k \geq l} b_k x^k$ be a power series with radius of convergence R , and let $\tilde{h}_l(x) = \sum_{k \geq l} |b_k| x^k$. For any matrix $A \in \mathbb{C}^{n \times n}$ with*

$\rho(A) < R$, if a_k is an upper bound for $\|A^k\|$ ($\|A^k\| \leq a_k$), $p \in \mathbb{N}$, $1 \leq p \leq l$, $p_0 \in \mathbb{N}$ is the multiple of p with $l \leq p_0 \leq l + p - 1$, and

$$\alpha_p = \max\{a_k^{\frac{1}{k}} : k = p, l, l+1, l+2, \dots, p_0-1, p_0+1, p_0+2, \dots, l+p-1\}, \quad (23)$$

then

$$\|h_l(A)\| \leq \tilde{h}_l(\alpha_p). \quad (24)$$

Using Theorem 1 the following theorem provides a sharper bound than (6) given originally by [34] for the remainder $R_m(W)$ of the matrix exponential Taylor series of nonnormal matrices.

Theorem 2. Let $A \in \mathbb{C}^{n \times n}$ be a square matrix and let $m \in \mathbb{N}$. Suppose that for each $k \in \mathbb{N}$, there exists an upper bound a_k such that $\|A^k\|_1 \leq a_k$. Let $p \in \mathbb{N}$ with $1 \leq p \leq m + 1$, and let p_0 be the multiple of p satisfying $m + 1 \leq p_0 \leq m + 1 + p$. Define

$$\alpha_p = \max\left\{a_k^{1/k} : k = p, m + 1, m + 2, \dots, p_0 - 1, p_0 + 1, p_0 + 2, \dots, m + 1 + p\right\}. \quad (25)$$

Then the remainder of the matrix exponential Taylor approximation of degree m ,

$$R_m(A) = e^A - \sum_{k=0}^m \frac{A^k}{k!} = \sum_{k=m+1}^{\infty} \frac{A^k}{k!}, \quad (26)$$

satisfies the bound

$$\|R_m(A)\|_1 < \frac{\alpha_p^{m+1}}{(m+1)!} \cdot \left(\frac{1}{1 - \frac{\alpha_p}{m+2}}\right), \quad (27)$$

provided that condition

$$\alpha_p < m + 2, \quad (28)$$

is fulfilled.

Proof. Let $A \in \mathbb{C}^{n \times n}$ be a square matrix and let $m \in \mathbb{N}$. The remainder of the matrix exponential Taylor approximation of degree m given by (5)

$$R_m(A) = e^A - T_m(A) = \sum_{k=m+1}^{\infty} \frac{A^k}{k!}.$$

Define the scalar power series

$$h_{m+1}(x) = \sum_{k=m+1}^{\infty} \frac{x^k}{k!} = \tilde{h}_{m+1}(x) = \sum_{k=m+1}^{\infty} \left| \frac{1}{k!} \right| x^k,$$

which has infinite radius of convergence. Suppose that for each $k \in \mathbb{N}$, there exists an upper bound $a_k \geq 0$ such that $\|A^k\|_1 \leq a_k$.

Let $p \in \mathbb{N}$ with $1 \leq p \leq m+1$, and let p_0 be the multiple of p satisfying $m+1 \leq p_0 \leq m+1+p$. Define

$$\alpha_p = \max \left\{ a_k^{1/k} : k = p, m+1, m+2, \dots, p_0-1, p_0+1, p_0+2, \dots, m+1+p \right\}.$$

By Theorem 1, we have

$$\|R_m(A)\|_1 = \left\| \sum_{k=m+1}^{\infty} \frac{A^k}{k!} \right\|_1 \leq \sum_{k=m+1}^{\infty} \frac{\|A^k\|_1}{k!} \leq \sum_{k=m+1}^{\infty} \frac{a_k}{k!} \leq \tilde{h}_{m+1}(\alpha_p). \quad (29)$$

To bound $\tilde{h}_{m+1}(\alpha_p)$, note that factoring out the first term one gets

$$\tilde{h}_{m+1}(x) = \frac{x^{m+1}}{(m+1)!} \cdot \sum_{k=0}^{\infty} \frac{x^k}{(m+2)(m+3) \cdots (m+1+k)}.$$

Note that for each $k \geq 0$,

$$(m+2)(m+3) \cdots (m+1+k) > (m+2)^k,$$

so

$$\frac{x^k}{(m+2)(m+3) \cdots (m+1+k)} < \left(\frac{x}{m+2} \right)^k.$$

Therefore,

$$\tilde{h}_{m+1}(x) < \frac{x^{m+1}}{(m+1)!} \cdot \sum_{k=0}^{\infty} \left(\frac{x}{m+2} \right)^k.$$

This is a geometric series with ratio $\frac{x}{m+2}$, and if $\frac{x}{m+2} < 1$ it converges to

$$\sum_{k=0}^{\infty} \left(\frac{x}{m+2} \right)^k = \frac{1}{1 - \frac{x}{m+2}}.$$

Hence,

$$\sum_{k=m+1}^{\infty} \frac{x^k}{k!} = \tilde{h}_{m+1}(x) < \frac{x^{m+1}}{(m+1)!} \cdot \frac{1}{1 - \frac{x}{m+2}}, \quad \text{for } x < m+2. \quad (30)$$

Applying (29) and (30) with $x = \alpha_p < m+2$ then (27) holds. \square

In the following, The matrix exponential scaling parameter, s , is determined based on the result of Theorem 2 to ensure that the Taylor series remainder remains below a predefined error tolerance. Let W be the weight matrix for generative flows from Algorithm 1. Let a_k be an upper bound for $\|W^k\|_1$ such that $\|W^k\|_1 \leq a_k$. Let $p \in \mathbb{N}$ with $1 \leq p \leq m+1$, and let p_0 be the multiple of p satisfying $m+1 \leq p_0 \leq m+1+p$. Let α_p be defined by (25). Let's scale the the matrix W by the scaling parameter s so that

$$\frac{\|(W/2^s)^{m+1}\|_1}{(m+1)!} \leq \frac{(\alpha_p/2^s)^{m+1}}{(m+1)!} \leq \varepsilon, \quad (31)$$

where ε is the selected user error tolerance from Algorithm 1. Note that ε must fulfill

$$\varepsilon \geq u, \quad (32)$$

where u is the machine unit roundoff error in the working precision arithmetic, since errors below the machine roundoff error can't be guaranteed in the working precision arithmetic computations. Then, if s fulfills (31) one gets

$$s \geq \frac{1}{m+1} \log_2 \left(\frac{\alpha_p^{m+1}}{(m+1)! \cdot \varepsilon} \right), \quad (33)$$

and then it follows that

$$s = \left\lceil \frac{1}{m+1} \log_2 \left(\frac{\alpha_p^{m+1}}{(m+1)! \cdot \varepsilon} \right) \right\rceil. \quad (34)$$

Since s is the lowest integer satisfying (34), then scaling the matrix W by s given by (34) it follows that

$$\frac{\|(W/2^s)^{m+1}\|_1}{(m+1)!} \leq \frac{(\alpha_p/2^s)^{m+1}}{(m+1)!} = \varepsilon' \leq \varepsilon, \quad (35)$$

and by (27) from Theorem 2, if $\alpha_p/2^s < m + 2$ one gets

$$\|R_m(W/2^s)\|_1 \leq \varepsilon' \frac{1}{1 - \frac{\alpha_p/2^s}{m+2}}, \quad (36)$$

where $\alpha_p/2^s = \varepsilon'^{\frac{1}{m+1}} \leq \varepsilon^{\frac{1}{m+1}}$ and then

$$\|R_m(W/2^s)\|_1 \leq \varepsilon \frac{1}{1 - \frac{\varepsilon^{1/m+1}}{m+2}}. \quad (37)$$

We verify the fulfillment of condition (28) by utilizing the error tolerance $\varepsilon = 10^{-8}$ reported in [25, Sec. 6.4] and the selected Taylor degrees $m \in \{1, 2, 4, 8, 15\}$ (as defined in Section 3.1). For these parameters, it is easy to show that the condition is satisfied since the maximum value of the bound, $\alpha_p/2^s$, meets the requirement

$$\alpha_p/2^s \leq \varepsilon^{\frac{1}{m+1}} = (10^{-8})^{\frac{1}{m+1}} < m + 2,$$

for each value of m . Subsequently, analyzing the maximum total error bound given by (36), we find it equals

$$\varepsilon + 1.75682 \times 10^{-18},$$

where the second term is approximately ten orders of magnitude smaller than the target tolerance ε . This effectively means the total error bound is dominated by ε , validating the scaling parameter selection derived from equation (34) under practical floating-point arithmetic.

To ensure that the bound is accomplished properly the proposed algorithm will compute the scaling parameter s by using the term $m + 1$ as stated here, and also the term $m + 2$, selecting the largest scaling parameter among both of them. For the case $m = 15+$, where the term $m + 1 = 16$ is not exactly $1/16!$, selecting the maximum scaling parameter obtained with $m + 1$ and also the term $m + 2 = 17$, for which the exponential remainder term corresponds effectively to $1/17!$, will ensure a proper scaling parameter value.

The error analysis for (8) is analogous to the error analysis described here, and the following theorem can be proved similarly:

Theorem 3. *Let $A \in \mathbb{C}^{n \times n}$ be a square matrix and let $m \in \mathbb{N}$. Suppose that for each $k \in \mathbb{N}$, there exists an upper bound a_k such that $\|A^k\|_1 \leq a_k$.*

Let $p \in \mathbb{N}$ with $1 \leq p \leq m + 1$, and let p_0 be the multiple of p satisfying $m + 1 \leq p_0 \leq m + 1 + p$. Define

$$\alpha_p = \max \left\{ a_k^{1/k} : k = p, m + 1, m + 2, \dots, p_0 - 1, p_0 + 1, p_0 + 2, \dots, m + 1 + p \right\}. \quad (38)$$

Then the remainder of the matrix exponential Taylor approximation of degree m ,

$$R'_m(A) = \sum_{k=m+1}^{\infty} \frac{A^k}{(k+1)!}, \quad (39)$$

satisfies the bound

$$\|R'_m(A)\|_1 < \frac{\alpha_p^{m+1}}{(m+2)!} \cdot \left(\frac{1}{1 - \frac{\alpha_p}{m+3}} \right), \quad (40)$$

provided that condition

$$\alpha_p < m + 3, \quad (41)$$

is fulfilled.

Finally, regarding the approximation in (8), we set the scaling parameter to $s = 0$, consistent with the approach described in [25, Sec. 3.2]. For Taylor based approximations of approximation orders $m \in \{1, 2, 4, 8, 15+\}$, we employ the efficient evaluation formulas detailed in Section 3.1. For degrees exceeding these values, we utilize the classical Paterson–Stockmeyer method.

3.3. Proposed algorithms

Taking into account the evaluation formulas from Section 3.1 and the error analysis from Section 3.2, Algorithm 2 computes the matrix exponential using the scaling and squaring algorithm and the Taylor polynomial approximation. Polynomials are efficiently evaluated by means of Paterson–Stockmeyer method or evaluation formulas (10)-(17). Error tolerance ε is variable, but it will be fixed to 10^{-8} in the experiments.

The algorithm is fundamentally suitable for any error tolerance ε that is greater than or equal to the unit roundoff error. However, note that when employing IEEE double precision arithmetic, where $u = 2^{-53} \approx 1.11 \times 10^{-16} \ll 10^{-8}$, to achieve a higher level of accuracy that approaches the machine precision the algorithm parameters should be adjusted. Specifically, the accuracy

Algorithm 2 Algorithm for Computing Matrix Exponential

Require: Weight matrix W , error tolerance ε

Ensure: Matrix exponential e^W

- 1: Obtain the polynomial order m and the scaling parameter s by using Algorithms 3 or 4
 - 2: $W = W/(2^s)$
 - 3: Evaluate the matrix polynomial $X = P_m(W)$ by Paterson-Stockmeyer technique or by evaluation formulas (10)-(17)
 - 4: **for** $i = 1$ **to** s **do**
 - 5: $X = X \cdot X$
 - 6: **end for**
 - 7: **return** X
-

is improved by selecting more terms in the Taylor approximation as shown in [22, Sec. 6].

Initially, Algorithm 2 determines the optimal parameters m and s by invoking Algorithm 3 or Algorithm 4. Next, the matrix W is scaled following the scaling and squaring approximation to reduce its norm. Then, the matrix polynomial is evaluated either using the Paterson–Stockmeyer method or evaluation formulas (10)-(17). Finally, the exponential of the matrix W is recovered carrying out the appropriate s matrix products corresponding to the squaring stage.

In the implemented functions derived from Algorithms 2, 3, and 4, \log_2 has been used to avoid the appearance of large numbers when computing high powers of α_p and factorials in expressions like (34), especially if low precision arithmetic is used.

As said above, the algorithm for evaluating (8) is analogous to Algorithm 2, setting $s = 0$ and using similar evaluation formulas to those in Section 3.1 for Taylor based approximations with $m = 1, 2, 4, 8, 15+$ and the Paterson–Stockmeyer method for Taylor approximations of degrees higher than 15+.

Algorithm 3 determines the polynomial order m and the scaling parameter s required to compute the matrix exponential of W using a Taylor approximation of order $m \leq 16$ and a desired tolerance ε . It is assumed that the polynomials are evaluated using the Paterson–Stockmeyer method.

Algorithm 3 Algorithm for Obtaining a Polynomial Order m and a Scaling Parameter s . The polynomial will be evaluated via Paterson–Stockmeyer

Require: Weight matrix W , error tolerance ε

Ensure: Polynomial order m and scaling parameter s

```

1:  $m = 0, s = 0$ 
2: if  $\|W\|_1 = 0$  then
3:   return  $m, s$ 
4: end if
5:  $M = [1, 2, 4, 6, 9, 12, 16]$ 
6:  $J = \lceil \sqrt{M} \rceil$ 
7:  $K = M./J$ 
8:  $C = [1./[2!, 3!, 3!, 4!, 5!, 6!, 7!, 8!, 10!, 11!, 13!, 14!, 17!, 18!]]$ 
9:  $finish = 0$ 
10:  $i = 1$ 
11: while  $i \leq \text{length}(M)$  and  $finish = 0$  do
12:    $m = M_i$ 
13:    $j = J_i$ 
14:    $k = K_i$ 
15:    $p = 2 \cdot i - 1$ 
16:   if  $m = 1$  then
17:      $E_1 = C_p \cdot \|W\|_1^2$ 
18:      $E_2 = C_{p+1} \cdot \|W\|_1^3$ 
19:   else
20:      $E_1 = C_p \cdot \|W^j\|_1^k \cdot \|W\|_1$ 
21:      $E_2 = C_{p+1} \cdot \|W^j\|_1^k \cdot \|W^2\|_1$ 
22:   end if
23:   if  $E_1 + E_2 \leq \varepsilon$  then
24:      $finish = 1$ 
25:   else
26:      $i = i + 1$ 
27:   end if
28: end while
29: if  $finish = 0$  then
30:   for  $i = 1$  to 2 do
31:      $s1 = \lceil \log_2(E_i/\varepsilon)/(m + i) \rceil$ 
32:     if  $s1 > s$  then
33:        $s = s1$ 
34:     end if
35:   end for
36: end if
37: if  $s > 20$  then
38:    $s = 20$ 
39: end if
40: return  $m, s$ 

```

Initially, if W is a null matrix, the values of m and s equal to 0 will be returned. Next, vector M stores the possible degrees of the considered polynomials, vector J is completed as the power of W that must be computed for each value of M , and vector K is filled in according to the quotient of the elements of M divided by the elements of J .

For each possible value m in M , vector C stores two consecutive values corresponding to the coefficients of the Taylor series located at positions $m+1$ and $m+2$, that is, $1/(m+1)!$ and $1/(m+2)!$.

Next, from lines 9 to 28, an attempt is made to determine the most appropriate degree m of the polynomial to use, from the point of view of accuracy and computational efficiency. Since $\frac{W^{m+1}}{(m+1)!}$ and $\frac{W^{m+2}}{(m+2)!}$ are the first two terms of the remainder for the Taylor-based approximation of order m to the exponential of W , our objective is to obtain the value of m that guarantees that:

$$\frac{\|W^{m+1}\|_1}{(m+1)!} + \frac{\|W^{m+2}\|_1}{(m+2)!} \leq \varepsilon, \quad (42)$$

where E_1 corresponds to the first summand and E_2 to the second one in the algorithm.

Notwithstanding, since W^{m+1} and W^{m+2} are not explicitly calculated, the 1-norm of these matrix powers is bounded using the 1-norm of the highest power of W computed thus far. For example, when $m = 1$ (lines 16–18), W is known, but $\|W^2\|_1$ and $\|W^3\|_1$ are required; these are bounded by $\|W\|_1^2$ and $\|W\|_1^3$, respectively. Similarly, if $m = 12$ (lines 19–21), W^4 has been previously calculated, and the required norms $\|W^{13}\|_1$ and $\|W^{14}\|_1$ are bounded by $\|W^4\|_1^3 \cdot \|W\|_1$ and $\|W^4\|_1^3 \cdot \|W^2\|_1$. Thus, if m equals 12, j and k take the values 4 and 3, accordingly.

If expression (42) is not satisfied for any considered value of m , then m is set equal to the maximum degree in vector M , i.e., $m = 16$. Consequently, the minimum value of s is obtained such that

$$\max \left(\frac{1}{(m+1)!} \cdot \left\| \left(\frac{W}{2^s} \right)^{m+1} \right\|_1, \frac{1}{(m+2)!} \cdot \left\| \left(\frac{W}{2^s} \right)^{m+2} \right\|_1 \right) \leq \varepsilon. \quad (43)$$

By solving for s in the first and second terms of (43) independently and taking the logarithm of each, we obtain

$$s \geq \max \left(\frac{1}{m+1} \cdot \log_2 \left(\frac{\|W^{m+1}\|_1}{\varepsilon \cdot (m+1)!} \right), \frac{1}{m+2} \cdot \log_2 \left(\frac{\|W^{m+2}\|_1}{\varepsilon \cdot (m+2)!} \right) \right), \quad (44)$$

in accordance with lines 30 to 36 in the algorithm. Finally, to avoid over-scaling, the maximum value of s is set to 20 in lines 37 and 38.

Similarly, Algorithm 3 fulfills the same role as Algorithm 2, but incorporates formulas (10)-(17) for evaluating the matrix polynomials. While the structure remains consistent with the previous algorithm, the polynomial degrees differ. Furthermore, the maximum explicitly computed power of W is restricted to W^2 . A key distinction lies in the penultimate value of vector C , which corresponds to the Taylor-based approximation T_{15+} defined in (17). As previously noted, this approximation is equivalent to (18), where b_{16} is given in IEEE double-precision arithmetic by (20). Consequently, the penultimate element of vector C is derived from the corresponding remainder term (19). For $m = 15$, the indices j and k are set to 2 and 8, respectively. Thus, using W^2 , the bounds for $\|W^{16}\|_1$ and $\|W^{17}\|_1$ (lines 20, 21, and 26) are bounded by $\|W^2\|_1^8$ and $\|W^2\|_1^8 \cdot \|W\|_1$. The calculation of the scaling parameter s follows the procedure described in Algorithm 2. However, in this case determining s based on the maximum value from the first two terms of the remainder (19) ensures a more conservative selection.

Algorithm 4 Algorithm for Obtaining an Polynomial Order m and a Scaling Parameter s . The polynomial will be evaluated via evaluation formulas (10)-(17)

Require: Weight matrix W , error tolerance ε

Ensure: Polynomial order m and scaling parameter s

```

1:  $m = 0, s = 0$ 
2: if  $\|W\|_1 = 0$  then
3:   return  $m, s$ 
4: end if
5:  $M = [1, 2, 4, 8, 15]$ 
6:  $J = [1, 2, 2, 2, 2]$ 
7:  $K = \lceil M./J \rceil$ 
8:  $C = [1/2!, 1/3!, 1/3!, 1/4!, 1/5!, 1/6!, 1/9!, 1/10!, |1/16! - b_{16}|, 1/17!] \triangleright b_{16}$ 
   from (20)
9:  $finish = 0$ 
10:  $i = 1$ 
11: while  $i \leq \text{length}(M)$  and  $finish = 0$  do
12:    $m = M_i$ 
13:    $j = J_i$ 
14:    $k = K_i$ 
15:    $p = 2 \cdot i - 1$ 
16:   if  $m = 1$  then
17:      $E_1 = C_p \cdot \|W\|_1^2$ 
18:      $E_2 = C_{p+1} \cdot \|W\|_1^3$ 
19:   else
20:      $E_1 = C_p \cdot \|W^j\|_1^k$ 
21:      $E_2 = C_{p+1} \cdot \|W^j\|_1^k$ 
22:     if  $j \cdot k = m$  then
23:        $E_1 = E_1 \cdot \|W\|_1$ 
24:        $E_2 = E_2 \cdot \|W^2\|_1$ 
25:     else
26:        $E_2 = E_2 \cdot \|W\|_1$ 
27:     end if
28:   end if
29:   if  $E_1 + E_2 \leq \varepsilon$  then
30:      $finish = 1$ 
31:   else
32:      $i = i + 1$ 
33:   end if
34: end while
35: if  $finish = 0$  then
36:   for  $i = 1$  to 2 do
37:      $s1 = \lceil \log_2(E_i/\varepsilon)/(m + i) \rceil$ 
38:     if  $s1 > s$  then
39:        $s = s1$ 
40:     end if

```

4. Numerical results

This section compares the numerical and computational properties of the different implementations. Following the baseline method in [25], we set the error tolerance to $\varepsilon = 10^{-8}$. The code is available at <https://github.com/hipersc/MatrixFunctions/>.

In all experiments, the normwise relative error serves as our primary metric to quantify the accuracy of each matrix exponential method relative to the “exact” solution (computed to double-precision limits, as detailed below). This error is defined as:

$$\text{Er}(A) = \frac{\|\exp(A) - \widetilde{\exp}(A)\|_2}{\|\exp(A)\|_2}, \quad (45)$$

where $\exp(A)$ and $\widetilde{\exp}(A)$ stands for the approximated and the “exact” solution.

In this section, all computational tests were conducted on a PC equipped with an Intel Core i9-14900HX processor, 32 GB of RAM, and an NVIDIA GeForce RTX 4070 graphics card. Comparisons were performed initially in MATLAB (version 2025a) and subsequently in PyTorch.

4.1. Numerical results in MATLAB

The numerical experiments are conducted against two primary benchmarks: the Taylor-based approach described in [25] (Algorithm 1) and a custom implementation of the Paterson–Stockmeyer (P–S) scheme. This selection is predicated on the current state of deep learning frameworks such as PyTorch, where native matrix exponential routines (e.g., `torch.linalg.expm`) are typically optimized for fixed IEEE precision formats and do not support user-defined variable error tolerances. Since [25] serves as the established reference for matrix exponential applications within generative flow models, it constitutes the appropriate baseline for assessing improvements in this specific domain. Furthermore, the inclusion of the P–S scheme as a secondary benchmark allows for a direct quantification of the efficiency gains attributable specifically to the advanced polynomial evaluation formulas integrated into the proposed algorithm.

To facilitate the comparison, the following three implementations were developed in MATLAB:

1. `expm_flow_ps`: An implementation based on the proposed Algorithm 2, where matrix polynomials are evaluated using the Paterson–Stockmeyer technique.
2. `expm_flow_sastre`: A version identical to the previous implementation, but utilizing evaluation formulas (10)-(17) for matrix polynomials.
3. `expm_flow`: The original algorithm proposed in [25], rewritten in MATLAB to ensure a fair comparison within the same computational environment.

To evaluate the performance of these three codes, a testbed composed of 360 ill-conditioned matrices belonging to the Matrix Computation Toolbox (MCT) [35] the Eigtool MATLAB Package (EMP) [36] was generated. Their size, always a power of 2, ranged from 4 to 1024. The “exact” exponential function of each matrix A was calculated, where applicable, following the three steps outlined in the following procedure:

- By applying the MATLAB function `eig` to the input matrix A , the matrices D and V were obtained such that $A = V \cdot D \cdot V^{-1}$. The matrix $E_1 = V \cdot \exp(D) \cdot V^{-1}$ was then generated.
- The matrix $E_2 = \exp(A)$ was derived using the MATLAB `expm` function, along with MATLAB Symbolic Math Toolbox and the function `vpa` (variable-precision floating-point arithmetic) with 256 decimal digits.
- Matrix E_1 was considered the “exact” exponential of A if the following condition holds:

$$\frac{\|E_1 - E_2\|_2}{\|E_1\|_2} \leq u,$$

where $u = 2^{-53}$ stands for the unit roundoff in IEEE double precision arithmetic. Otherwise, matrix A was excluded.

Graphically, Figure 1 shows the results obtained from the first of the experiments, carried out on the matrices comprising MCT and EMP. Figure 1a displays the normwise relative error committed by each of the codes for the different matrices analysed. These same errors, ordered from highest to lowest for code `expm_flow_sastre`, are also shown in Figure 1b. The black line appearing in 1a corresponds to the expected relative error when

calculating the exponential of the matrices. This value is equivalent to the product of the condition number of the exponential function for each matrix multiplied by the error tolerance used (10^{-8}) in our experiments. Ideally, it is to be expected that all results will be below this line, with those ones further down clearly being better. It is easy to see how the results for `expm_flow` are less accurate than those for `expm_flow_sastre` and `expm_flow_ps`, as they occupy the highest positions in the graph.

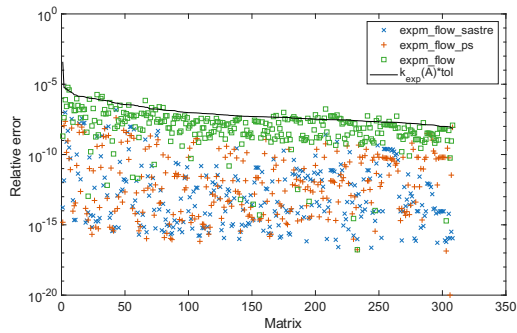
Figure 1c corresponds to the performance profile. It represents, for each value α on the x -axis, the percentage of matrices, expressed as a proportion of one, for which the error incurred in calculating their exponential function is α times less than or equal to the minimum error committed by each of the methods compared. The higher the values provided, the better the code. As we can appreciate, `expm_flow_sastre` and `expm_flow_ps` occupy the top of the picture, while `expm_flow` provides the poorest results. While `expm_flow_ps` offers better results for α equal to 1, this improvement is reversed in favour of `expm_flow_sastre` from α values close to 4.

The direct correspondence of these values for α equal to 1 are those ones collected, in the form of a pie chart, on the left side of Figure 1d. It represents the percentage of cases in which each code yielded the most accurate result. Thus, we can state that `expm_flow_ps` provided the closest values to the exact solution in 58% of cases, `expm_flow_sastre` in 42% of matrices, and `expm_flow` in a negligible percentage close to 0. In contrast, the right side of the picture reports the percentage of matrices for which each method gave the most inaccurate result. As we can see, `expm_flow` accounted for 99% of the matrices, clearly being the code with the worst performance.

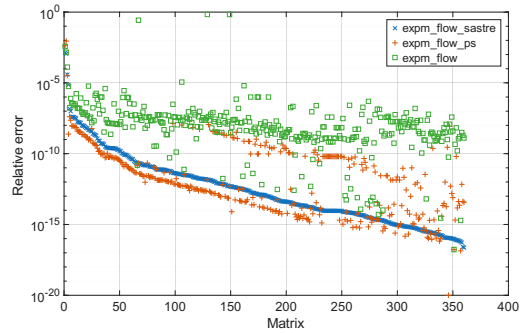
As whisker plots, Figures 1e and Figure 1f display respectively the order of the polynomial applied and the value of the parameter s used in the scaling and squaring technique. In each box, the red centre line indicates the median, and the blue bottom and top lines indicate the 25th and 75th percentiles, correspondingly. The whiskers extend to the most extreme data points that are not considered outliers, and outliers are represented individually by the “+” marker symbol. The code `expm_flow_ps` usually worked with polynomials of degree 16, or 15 in the case of `expm_flow_sastre`, while `expm_flow` used polynomials of lower order, in most cases between 5 and 7. Regarding the scaling parameter s , the median value was 1 for the code `expm_flow_ps`, 2 for `expm_flow_sastre`, and 5 for `expm_flow`. The maximum values reached were equal to 20 for `expm_flow_ps` and `expm_flow_sastre` and 718 for `expm_flow`.

Finally, Figures 1g and 1h present, in the form of a bar chart, two key comparative results: the number of matrix products required by each code and the response times (expressed in seconds) employed in the computation of all test matrices. Specifically, `expm_flow_ps` required 3,110 products, which is approximately 1.20 times the 2,597 products needed by the baseline `expm_flow_sastre`. The least efficient code, `expm_flow`, required 5,397 matrix products, representing a factor of approximately 2.08 compared to `expm_flow_sastre`. This comparison highlights `expm_flow_sastre` as the most product-efficient implementation, followed by `expm_flow_ps`, with `expm_flow` consistently requiring over twice the computational effort in terms of matrix multiplications.

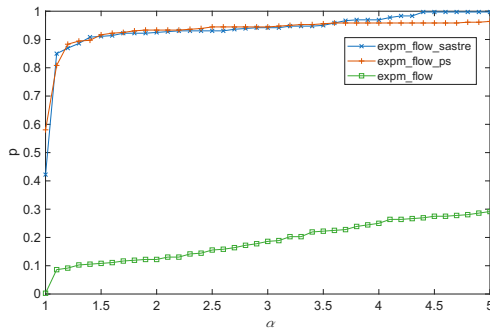
The analysis of execution times confirms the relative performance difference, using `expm_flow_sastre` as the baseline for comparison. Specifically, `expm_flow_ps` required 1.56 seconds for computation, making it approximately 1.13 times slower than the 1.39 seconds required by `expm_flow_sastre`. The least efficient code, `expm_flow`, required 2.31 seconds, resulting in a time factor of approximately 1.67 times slower compared to `expm_flow_sastre`. This comparison confirms `expm_flow_sastre` is the fastest implementation, with `expm_flow` exhibiting the largest runtime overhead. Notably, these execution time ratios are lower than the corresponding matrix product ratios. This reduced proportionality occurs because the test matrices, which range in size from 4×4 to 1024×1024 , are not all large enough for the number of computed matrix products to fully dominate the total execution cost.



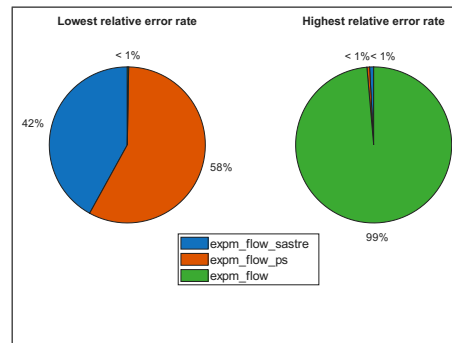
(a) Normwise relative error.



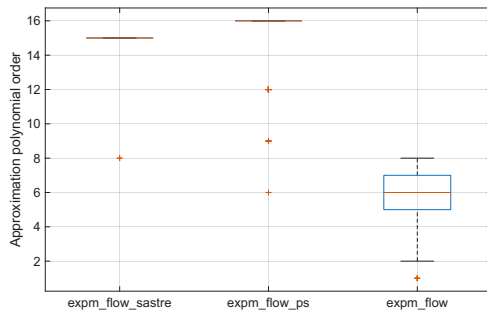
(b) Ordered normwise relative error.



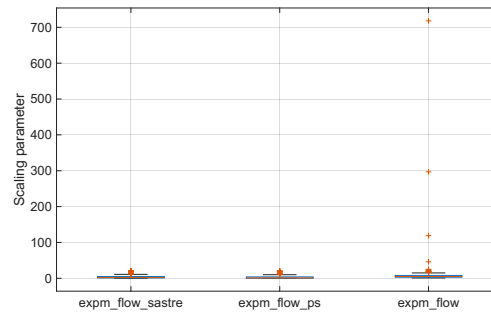
(c) Performance profile.



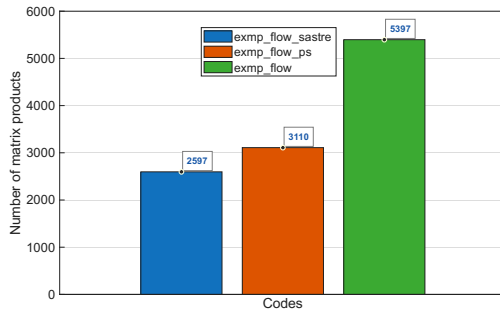
(d) Lowest and highest relative error rate.



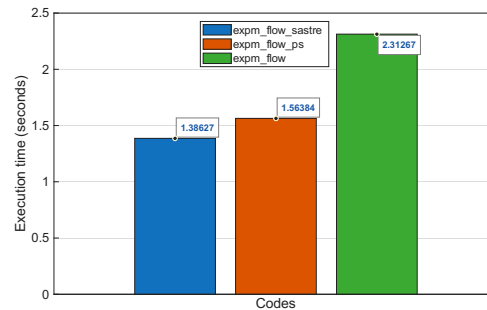
(e) Polynomial order.



(f) Scaling parameter.



(g) Number of matrix products.



(h) Execution time.

Figure 1: Experimental results for matrices in MCT and EMP sets.

4.2. Performance evaluation in the PyTorch generative flow environment

In this subsection, the results of tests performed directly on the code available in [25] will be described. As mentioned before, this code incorporates a matrix exponential function into neural networks implementing generative flows models. In our executions, the matrix exponential is computed using the following functions implemented in PyTorch:

1. `expm_flow_ps` is based on Algorithm 2 and evaluates the polynomial using the Paterson–Stockmeyer method.
2. `expm_flow_sastre`: Analogous to the previous function, this implementation is based on Algorithm 2, but the polynomials are evaluated using formulas (10)-(17).
3. `expm_flow` directly corresponds to the matrix exponential approximation method presented in [25].

All executions were carried out using CUDA and the graphics card of the machine involved. As testbeds in training, CIFAR-10 [37], ImageNet32 and ImageNet64 [38] datasets were used. The number of invocations analysed to extract results to the functions responsible for calculating the matrix exponential during the training process was 5000. For each call to the exponential function, multiple data were recorded for the matrices comprising the tensor to be computed, such as the number of matrices, their sizes, and the highest matrix ∞ -norm of all of them. Thus, we can confirm that the ∞ -norm of the matrices studied varied from $2.84e-4$ to 12.57 for CIFAR-10, from $1.17e-05$ to 12.49 for ImageNet32, and from $1.27e-05$ to 12.8 for ImageNet64.

In addition, the following metrics were logged for each of the three comparison functions: the degree of the polynomial used, the scaling parameter, the maximum error observed across all matrices in the tensor, the total number of matrix products involved, and the required response time.

When estimating the normwise relative error committed in the computation of each matrix in (45), it was assumed that `linalg.matrix_exp`, the PyTorch implementation of the exponential function, provides an exact solution.

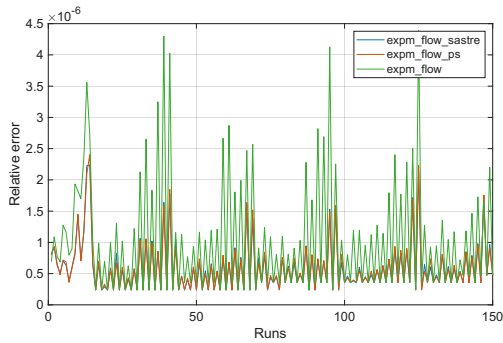
Figures 2, 3, and 4 graphically illustrate the results obtained for CIFAR-10, ImageNet32 and ImageNet64 datasets, respectively. Figures 2a, 3a, and 4a plot the normwise relative errors just for the first 150 training runs. For clarity, these same results are shown sorted, but now for the 5000 runs, from largest to smallest error independently for the three functions analysed in Figures 2b, 3b, and 4b. Unlike 1b, there is here no correspondence

between a matrix on the x -axis and the three errors that appear on the y -axis, due to the aforementioned sorting. As we can observe, `expm_flow` always resulted in higher errors in the exponential approximation. In contrast, `expm_flow_sastre` and `expm_flow_ps` provided very similar results, with `expm_flow_sastre` being slightly more accurate for the three datasets. This conclusion can also be deduced from the Figures 2c, 3c, and 4c related to the performance profile, where `expm_flow_sastre` and `expm_flow_ps` quickly provided probabilities equal to 1.

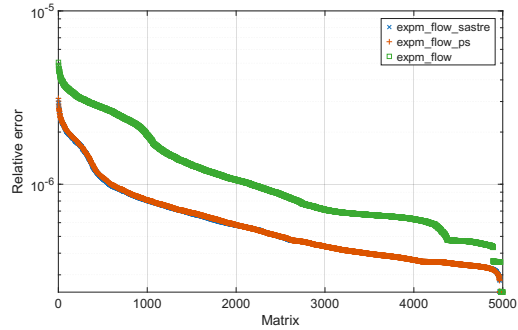
Figures 2d, 3d, and 4d also confirm that code `expm_flow_sastre` delivered a more accurate result than the other functions in a higher percentage of cases, with values of 50%, 49%, and 50% of the matrices for the three datasets, respectively. In turn, function `expm_flow_sastre` provided similar but slightly lower percentages, with values of 48%, for CIFAR-10, and 45%, for ImageNet32 and ImageNet64.

In clear accordance with Figures 1e, Figures 2e, 3e, and 4e also reveal that `expm_flow` used polynomials of a lower order than those of the other functions. In contrast, `expm_flow` required higher values of the scaling parameter, as can be appreciated in Figures 2f, 3f, and 4f.

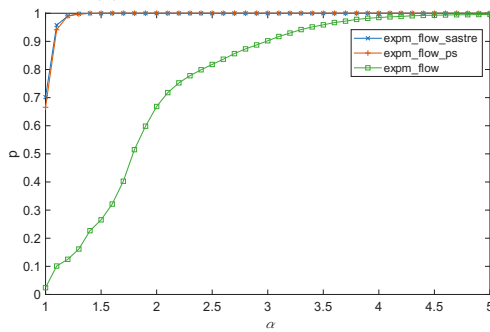
Finally, with regard to the number of products, Figures 2g, 3g, and 4g state that `expm_flow` carried out 1.99, 1.86, and 1.88 times more products than `expm_flow_sastre` in the calculation of matrix exponentials. Similarly, Figures 2h, 3h, and 4h show that the exponential computation based on function `expm_flow_sastre` was 1.87, 1.97, and 2.5 times faster than the same calculation using function `expm_flow`.



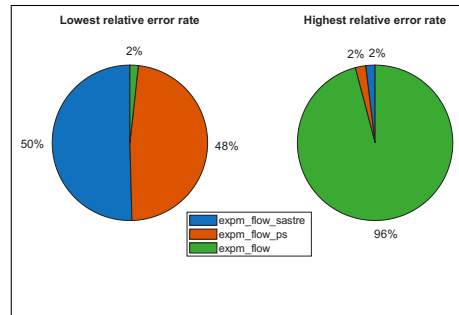
(a) Normwise relative error.



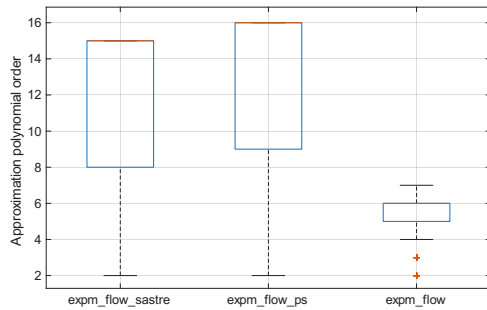
(b) Unmatched ordered normwise relative error.



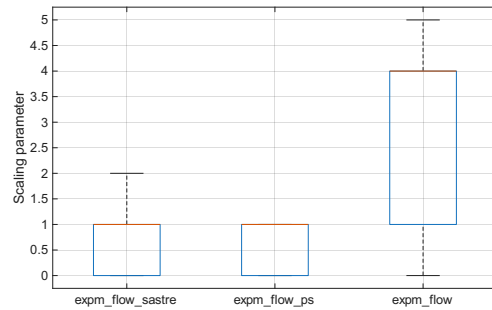
(c) Performance profile.



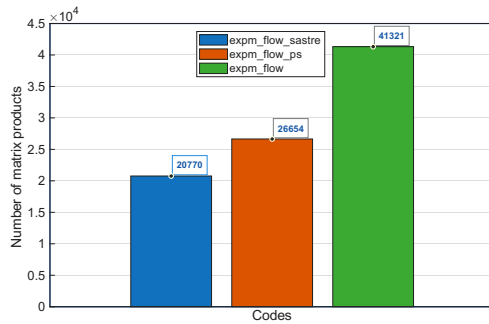
(d) Lowest and highest relative error rate.



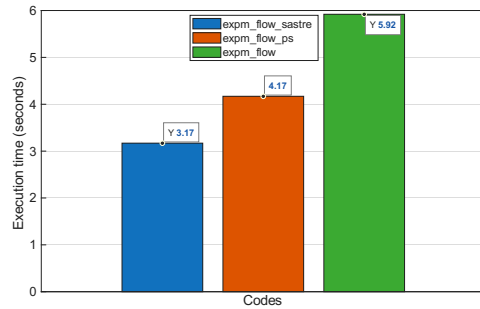
(e) Polynomial order.



(f) Scaling parameter.

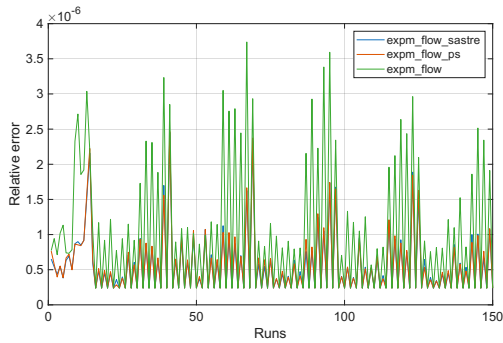


(g) Number of matrix products.

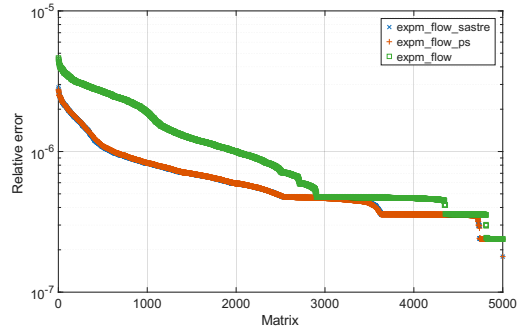


(h) Execution time.

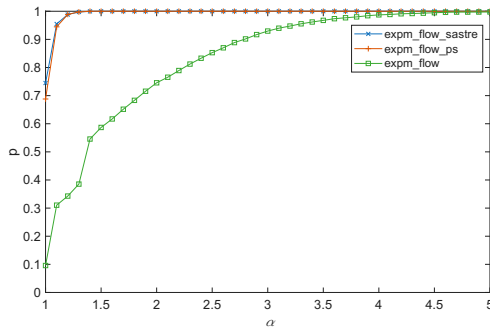
Figure 2: Experimental results for CIFAR10 dataset.



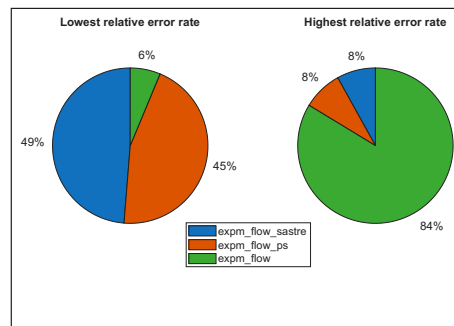
(a) Normwise relative error.



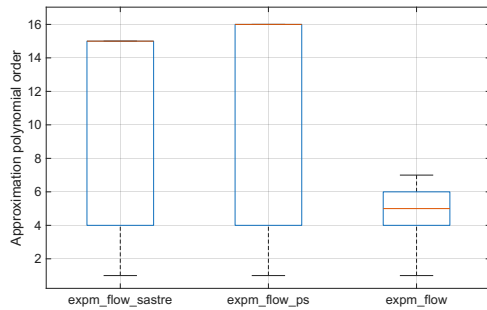
(b) Unmatched ordered normwise relative error.



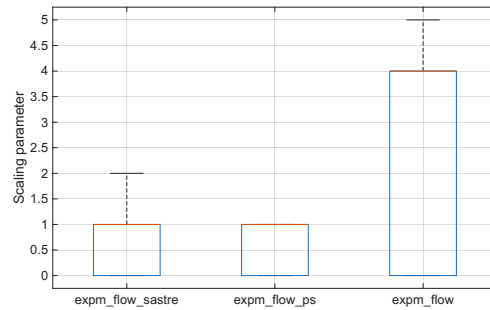
(c) Performance profile.



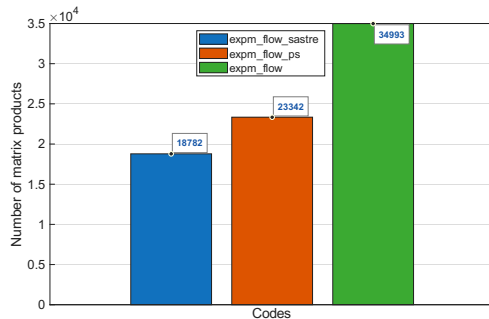
(d) Lowest and highest relative error rate.



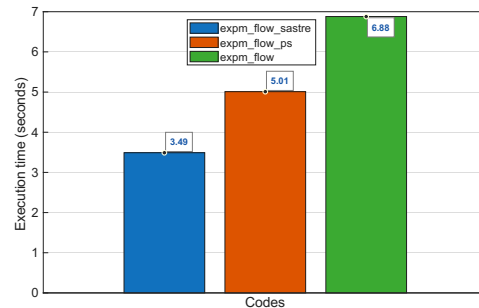
(e) Polynomial order.



(f) Scaling parameter.

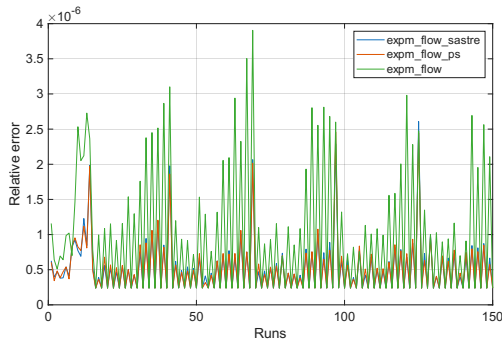


(g) Number of matrix products.

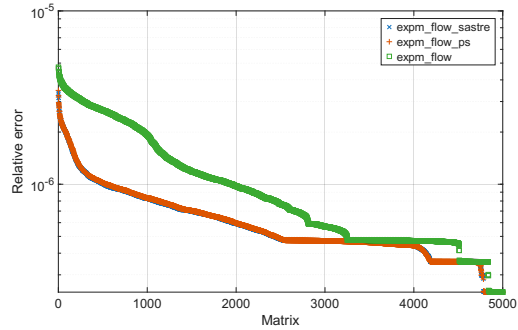


(h) Execution time.

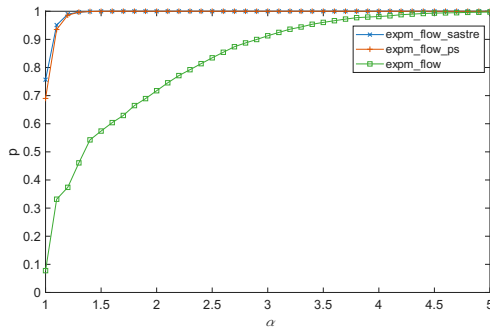
Figure 3: Experimental results for ImageNet32 dataset.



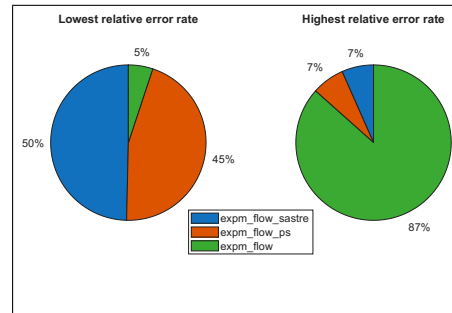
(a) Normwise relative error.



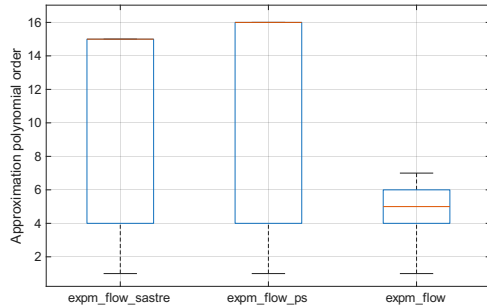
(b) Unmatched ordered normwise relative error.



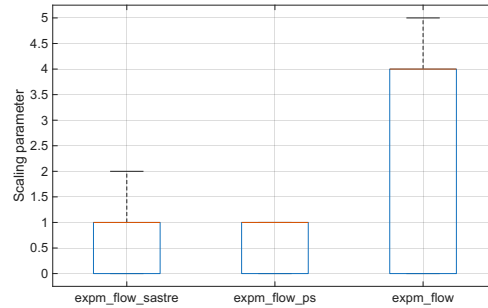
(c) Performance profile.



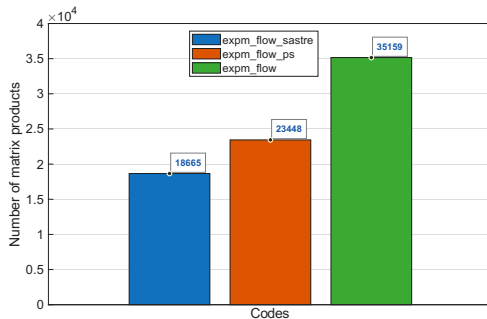
(d) Lowest and highest relative error rate.



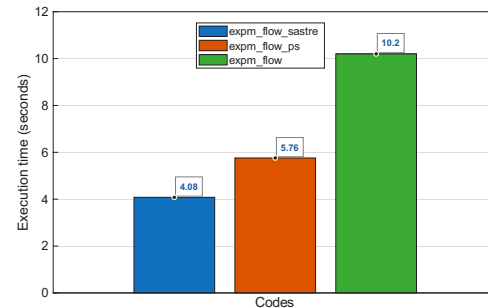
(e) Polynomial order.



(f) Scaling parameter.



(g) Number of matrix products.



(h) Execution time.

Figure 4: Experimental results for ImageNet64 dataset.

5. Performance analysis in generative flow models

To evaluate the efficiency gains of the proposed matrix exponential approach (`expm_flow_sastre`) relative to the baseline (`expm_flow`), we conducted a series of numerical experiments using three standard computer vision datasets: CIFAR-10, ImageNet32, and ImageNet64. All tests were executed on a system equipped with an Intel Xeon Platinum 8268 Processor, an NVIDIA RTX8000 GPU and 128 GB of RAM.

The evaluation consists of two parts. First, isolated benchmarks were performed to compare the execution times of both methods across various matrix sizes, independent of other neural network components. Second, both algorithms were integrated into the coupling layers of a Glow-based architecture [39], following the methodology described in [25]. Performance is quantified by measuring total computation time and calculating the speed-up ratio, defined as the execution time of `expm_flow` divided by that of `expm_flow_sastre`.

The flow model architecture, illustrated in Figure 5, follows a multi-scale structure. The squeeze operation performs downsampling by halving the spatial dimensions and quadrupling the channel count. Subsequently, the split operation partitions the feature maps along the channel dimension; one portion is directed to the output as a latent representation, while the remaining part is propagated through the subsequent layers of the model. Training was conducted for 50 epochs using the Adam optimizer [43] with a fixed learning rate of 0.01.

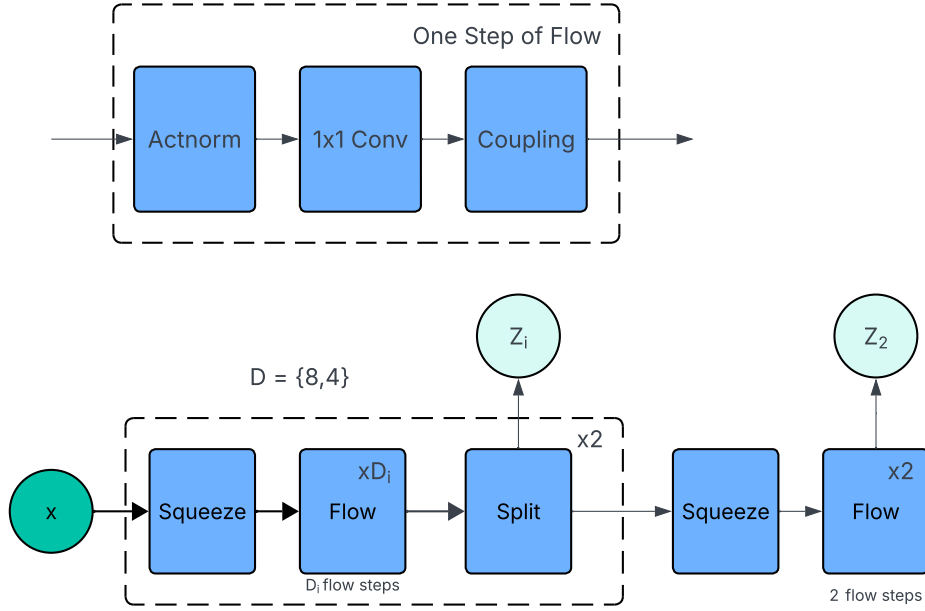


Figure 5: Diagram overview of flow model trained to generate images.

5.1. Computational scaling and matrix dimensionality

This analysis evaluates how the performance of the proposed matrix exponential implementation, `expm_flow_sastre`, scales relative to the baseline, `expm_flow`, as matrix dimensionality increases. We examine matrix orders $n \in \{8, 16, 32, 64, 128, 256, 512, 1024\}$ under two distinct scenarios: individual matrix transformations of size $n \times n$ and batched tensor operations of size $n \times 16 \times 16$. The execution time required to compute 1000 matrix exponentials was recorded for each configuration, with the resulting trends illustrated in Figure 6.

In both experimental setups, the relative efficiency of the proposed algorithm improves as the matrix order increases. A more pronounced performance gain is observed when varying the batch size compared to isolated changes in matrix dimensionality. This behavior stems from the fact that for

smaller matrices, such as 8×8 or 16×16 , the total execution cost is not yet dominated by the number of matrix products, as fixed computational overheads remain significant. As the dimensionality grows toward 1024×1024 , the computation becomes strictly limited by the number of matrix multiplications M . Consequently, the proposed method yields substantial benefits by reducing the required multiplication count, effectively leveraging the parallel linear algebra routines provided by the PyTorch backend, such as cuBLAS and MKL.

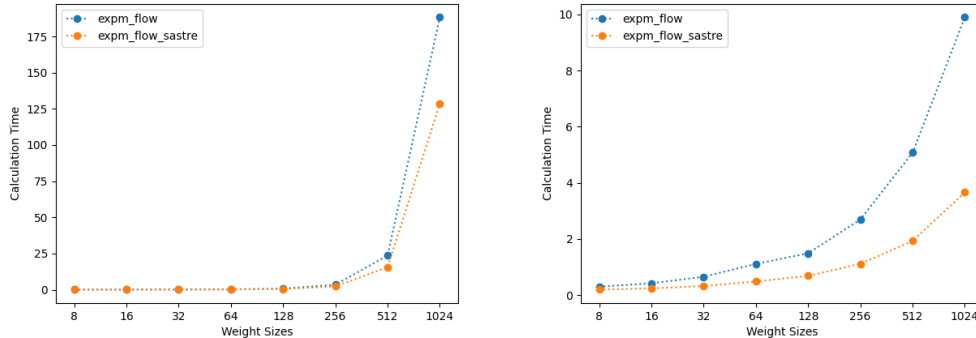


Figure 6: Comparison of the execution time required to calculate the matrix exponential using the original method (`expm_flow`) and the proposed method (`expm_flow_sastre`). The results are presented for different matrix sizes $n \in \{2, 4, 8, 16, 32, 64, 128, 256, 512, 1024\}$. (Left) Performance analysis for single $n \times n$ matrices. (Right) Performance analysis for tensors of size $n \times 16 \times 16$.

5.2. Training Performance and Scaling

To evaluate the practical utility of our approach, we integrated the proposed matrix exponential method into a generative framework. Glow [39] is a coupling layer approach to learning invertible transformations. We replaced the original implementation (`expm_flow`) with our optimized function (`expm_flow_sastre`) to measure its impact on computational efficiency during the training phase. All models were trained for 50 epochs across three benchmark datasets: CIFAR-10, ImageNet32, and ImageNet64. As detailed in Table 4, the proposed method demonstrates increased computational efficiency across all tested configurations. While the minimum observed speed-up was 3.91 for ImageNet64, the most significant gain occurred with ImageNet32, where training was nearly 10 times faster (9.74) than the baseline. This dramatic reduction in training time, specifically the shift from 32,304

seconds to 3,317 seconds per epoch on ImageNet32, demonstrates that the computational bottleneck previously associated with matrix exponentials in flow-based models can be effectively mitigated.

Dataset	CIFAR-10	ImageNet32	ImageNet64
<code>expm_flow</code> time	2463	32304	42482
<code>expm_flow_sastre</code> time	443.4	3317	10875
Speed-up	5.554	9.739	3.906

Table 4: Average training time per epoch (in seconds) for the matrix exponential version of Glow. Results compare the efficiency of our proposed `expm_flow_sastre` function against the original `expm_flow` implementation across three standard datasets.

5.3. Inference and Sampling Performance

While the previous sections evaluated performance during the training phase, efficiency during inference is equally critical for generative models. Table 5 presents a comparison of the sampling times between `expm_flow` and `expm_flow_sastre`. In this context, sampling time refers to the duration required for the model to generate an image from the latent space. We evaluated two scenarios: generating a single image ($n = 1$) and generating a batch of 128 images ($n = 128$). The results demonstrate that the speedup provided by our method becomes significantly more pronounced as the batch size increases. While the performance is nearly identical for a single sample, the `expm_flow_sastre` variant achieves a speedup factor of approximately 1.95 for larger batches, effectively halving the inference latency.

Sample	1 sample	128 samples
<code>expm_flow</code> time	0.3839	0.8286
<code>expm_flow_sastre</code> time	0.3836	0.4247
Speed-up	1.001	1.951

Table 5: Average inference times (in seconds) for sampling a matrix exponential variant of Glow. We compare the original `expm_flow` against `expm_flow_sastre` for single and batched samples, including the calculated speedup factor.

6. Conclusions

This work presented a Taylor-based algorithm for the computation of the matrix exponential, utilizing advanced polynomial evaluation schemes that extend beyond the classical Paterson–Stockmeyer technique. The proposed method incorporates a self-contained framework for the dynamic selection of the Taylor order and scaling factor, based on a rigorous error analysis designed to maintain accuracy for any user-specified tolerance ε greater than or equal to the working unit roundoff. This approach distinguishes itself from traditional implementations that rely on fixed-precision tables and from complex variable-precision algorithms that require specialized external libraries.

The algorithm was specifically evaluated within the context of generative AI flows, where the matrix exponential constitutes a primary computational requirement for modeling invertible transformations. By leveraging refined error bounds for nonnormal matrices and streamlined operational logic, the proposed method provides a more efficient alternative to previous dynamic schemes. Numerical evaluations conducted on both a diverse testbed of matrices and practical generative models demonstrate that, relative to the original implementation, the proposed Taylor-based approach yields training speedups between 3.91 and 9.74 while reducing inference latency by approximately 50% in large-batch scenarios.

These results demonstrate that modern polynomial evaluation strategies allow for higher-order approximations at a lower computational cost, measured in terms of matrix multiplications (M), than traditional rational or Paterson–Stockmeyer-based methods. Consequently, the proposed implementation offers a portable, library-independent solution for high-throughput applications and large-scale simulation environments.

Acknowledgements

The authors would like to thank Roger B. Dannenberg for providing valuable feedback on the writing of this manuscript.

Author contributions

J. Sastre: Conceptualization, Methodology, Software, Formal analysis, Funding acquisition, Project administration, Writing - original draft, Writing - review & editing.

D. Faronbi: Software, Validation, Investigation, Data curation, Resources, Visualization, Writing - original draft, Writing - review & editing.

J.M. Alonso: Methodology, Software, Formal analysis, Validation, Investigation, Data curation, Resources, Visualization, Writing - original draft, Writing - review & editing.

P. Traver: Software, Investigation, Validation, Resources, Visualization, Writing - review & editing.

J. Ibáñez: Methodology, Formal analysis, Investigation, Data curation, Visualization, Supervision, Writing - review & editing.

N. Lloret.: Resources, Validation, Supervision, Funding acquisition, Project administration, Writing - review & editing.

Declaration of competing interest

The authors declare that they have no known competing financial interests or personal relationships that could have appeared to influence the work reported in this paper.

Disclosure of generative AI and AI-assisted technologies in the writing process

During the preparation of this work the authors used Gemini in order to improve the language and readability of the manuscript. After using this tool, the authors reviewed and edited the content as needed and take full responsibility for the content of the published article.

7. References

References

- [1] N.J. Higham, *Functions of Matrices: Theory and Computation*, SIAM, Philadelphia, PA, 2008.
- [2] C.B. Moler, C.F. Van Loan, Nineteen dubious ways to compute the exponential of a matrix, twenty-five years later, *SIAM Rev.* 45 (2003) 3–49.
- [3] J. Sastre, J.J. Ibáñez, E. Defez, P.A. Ruiz, Efficient scaling-squaring Taylor method for computing matrix exponential, *SIAM J. Sci. Comput.* 37 (1) (2015) A439–A455.

- [4] J. Sastre, J. Ibáñez, E. Defez, P. Ruiz, Accurate matrix exponential computation to solve coupled differential models in engineering, *Math. Comput. Model.* 54 (2011) 1835–1840.
- [5] J. Sastre, J. Ibáñez, E. Defez, P. Ruiz, Accurate and efficient matrix exponential computation, *Int. J. Comput. Math.* 91 (1) (2014) 97–112.
- [6] P. Ruiz, J. Sastre, J. Ibáñez, E. Defez, High performance computing of the matrix exponential, *J. Comput. Appl. Math.* 291 (2016) 370–379.
- [7] J. Sastre, J. Ibáñez, P. Alonso, J. Peinado, E. Defez, Two algorithms for computing the matrix cosine function, *Appl. Math. Comput.* 312 (2017) 66–77.
- [8] E. Defez, J. Ibáñez, J. Sastre, J. Peinado, P. Alonso, A new efficient and accurate spline algorithm for the matrix exponential computation, *J. Comput. Appl. Math.* 296 (2017) 164–178.
- [9] J. Sastre, Efficient evaluation of matrix polynomials, *Linear Algebra Appl.* 539 (2018) 229–250.
- [10] J. Sastre, J. Ibáñez, Evaluation of matrix polynomials beyond the Paterson–Stockmeyer method, *Mathematics* 9 (2021) 1600.
- [11] J. Sastre, Efficient mixed rational and polynomial approximation of matrix functions, *Appl. Math. Comput.* 218 (24) (2012) 11938–11946.
- [12] S. Blackford, J. Dongarra, Installation guide for LAPACK, LAPACK Working Note 41, Univ. of Tennessee, 1999.
- [13] M.S. Paterson, L.J. Stockmeyer, On the number of nonscalar multiplications necessary to evaluate polynomials, *SIAM J. Comput.* 2 (1) (1973) 60–66.
- [14] P. Bader, S. Blanes, F. Casas, Computing the matrix exponential with an optimized Taylor polynomial approximation, *Mathematics* 7 (12) (2019) 1174.
- [15] S. Blanes, N. Kopylov, M. Seydaoğlu, Efficient Scaling and Squaring Method for the Matrix Exponential, *SIAM J. Matrix Anal. Appl.* 46 (1) (2025) 74–93.

- [16] M. Fasi, N.J. Higham, An Arbitrary Precision Scaling and Squaring Algorithm for the Matrix Exponential, *SIAM J. Matrix Anal. Appl.* 40 (4) (2019) 1233–1256.
- [17] M. Caliari, F. Zivcovich, On-the-fly backward error estimate for matrix exponential approximation by Taylor algorithm, *Appl. Math. Comput.* 338 (2018) 526–535.
- [18] E. Jarlebring, M. Fasi, E. Ringh, Computational graphs for matrix functions, *ACM Trans. Math. Softw.* 48 (4) (2023) 1–35.
- [19] E. Jarlebring, J. Sastre, J. Ibáñez, Polynomial approximations for the matrix logarithm with computation graphs, *Linear Algebra Appl.* 721 (2025) 692–714.
- [20] N.J. Higham, F. Tisseur, A block algorithm for matrix 1-norm estimation, with an application to 1-norm pseudospectra, *SIAM J. Matrix Anal. Appl.* 21 (2000) 1185–1201.
- [21] A.H. Al-Mohy, N.J. Higham, A new scaling and squaring algorithm for the matrix exponential, *SIAM J. Matrix Anal. Appl.* 31 (3) (2009) 970–989.
- [22] J. Sastre, J. Ibáñez, E. Defez, Boosting the computation of the matrix exponential, *Appl. Math. Comput.* 340 (2019) 206–220.
- [23] N.J. Higham, The scaling and squaring method for the matrix exponential revisited, *SIAM J. Matrix Anal. Appl.* 26 (4) (2005) 1179–1193.
- [24] E.D. Dolan, J.J. Moré, Benchmarking optimization software with performance profiles, *Math. Program.* 91 (2002) 201–213.
- [25] C. Xiao, L. Liu, Generative flows with matrix exponential, in: *Proc. 37th Int. Conf. Mach. Learn.*, PMLR, 2020, pp. 10452–10461.
- [26] J. Corwell, W.D. Blair, Industry Tip: Quick and Easy Matrix Exponentials, *IEEE Aerosp. Electron. Syst. Mag.* 35 (5) (2020) 49–52.
- [27] J. Copet, F. Kreuk, I. Gat, T. Remez, D. Kant, G. Synnaeve, Y. Adi, A. Défossez, Simple and controllable music generation, in: *Adv. Neural Inf. Process. Syst.*, vol. 36, 2023, pp. 47704–47720.

- [28] S.L. Wu, C. Donahue, S. Watanabe, N.J. Bryan, Music ControlNet: Multiple Time-Varying Controls for Music Generation, *IEEE/ACM Trans. Audio Speech Lang. Process.* 32 (2024) 2692–2703.
- [29] Y. Bengio, L. Yao, G. Alain, P. Vincent, Generalized denoising auto-encoders as generative models, in: *Adv. Neural Inf. Process. Syst.*, vol. 26, 2013.
- [30] A. Jahanian, X. Puig, Y. Tian, P. Isola, Generative models as a data source for multiview representation learning, 2021, arXiv:2106.05258.
- [31] I.J. Goodfellow, J. Pouget-Abadie, M. Mirza, B. Xu, D. Warde-Farley, S. Ozair, A. Courville, Y. Bengio, Generative adversarial nets, in: *Adv. Neural Inf. Process. Syst.*, vol. 27, 2014.
- [32] D.P. Kingma, M. Welling, Auto-encoding variational Bayes, 2013, arXiv:1312.6114.
- [33] J. Ho, A. Jain, P. Abbeel, Denoising diffusion probabilistic models, in: *Adv. Neural Inf. Process. Syst.*, vol. 33, 2020, pp. 6840–6851.
- [34] M. Liou, A novel method of evaluating transient response, *Proc. IEEE* 54 (1966) 20–23.
- [35] N.J. Higham, The Matrix Computation Toolbox, 2025. <https://es.mathworks.com/matlabcentral/fileexchange/2360-the-matrix-computation-toolbox> (accessed 22 December 2025).
- [36] T.G. Wright, Eigtool, version 2.1, 2009. <http://www.comlab.ox.ac.uk/pseudospectra/eigtool> (accessed 22 December 2025).
- [37] A. Krizhevsky, G. Hinton, Learning multiple layers of features from tiny images, Technical Report, University of Toronto, 2009.
- [38] A. van den Oord, N. Kalchbrenner, K. Kavukcuoglu, Pixel Recurrent Neural Networks, in: *Proc. 33rd Int. Conf. Mach. Learn.*, PMLR, 2016, pp. 1747–1756.
- [39] D.P. Kingma, P. Dhariwal, Glow: Generative flow with invertible 1x1 convolutions, in: *Adv. Neural Inf. Process. Syst.*, vol. 31, 2018.

- [40] G. Papamakarios, T. Pavlakou, I. Murray, Masked autoregressive flow for density estimation, in: *Adv. Neural Inf. Process. Syst.*, vol. 30, 2017.
- [41] L. Dinh, J. Sohl-Dickstein, S. Bengio, Density estimation using Real NVP, 2016, arXiv:1605.08803.
- [42] R.T.Q. Chen, J. Behrmann, D.K. Duvenaud, J.H. Jacobsen, Residual flows for invertible generative modeling, in: *Adv. Neural Inf. Process. Syst.*, vol. 32, 2019.
- [43] Z. Zhang, Improved Adam optimizer for deep neural networks, in: 2018 IEEE/ACM 26th Int. Symp. Qual. Serv. (IWQoS), 2018.